Statistical Assessment of High-Resolution Climate Model Rainfall Data in the Ciliwung Watershed, Indonesia

Widya Ningrum[1,3], Rizaldi Boer[2,3], Apip[1]

[1]National Research and Innovation Agency, Central Jakarta, Jakarta, Indonesia 10340
[2]Centre for Climate Risk and Opportunity Management in Southeast Asia Pacific, IPB University, Baranangsiang Campus, Bogor, Indonesia 16143
[3]Department of Geophysics and Meteorology, Faculty of Mathematics and Natural Sciences, IPB University, Dramaga Campus, Bogor, Indonesia 16680

Correspondence:
Widya Ningrum
National Research and Innovation Agency, Central Jakarta, Jakarta, Indonesia 10340
Email: widy011@brin.go.id

ABSTRACT

The impact of climate change on hydrometeorological hazards pointed out the necessity for information on rainfall data. Using Climate Hazard Group InfraRed Precipitation with Station (CHIRPS) data could solve the problem of the scarcity of observed rainfall data at a finer spatial resolution. This paper examines the performance of high-resolution rainfall climate model data called CORDEX SEA and NEXGDPP in the Ciliwung watershed, Indonesia. We used CHIRPS data as observed data, which was separately divided for calibration (1981-2005) and validation (2006-2020) of the climate models. Totally 14 climate models were used, comprised of 4 CORDEX and 10 NEXGDPP. The models accuracy was assessed based on three statistical indicators: bias, mean absolute percentage error (MAPE), and mean square error (MSE). We determined the best model based on Taylor Diagram. The results showed that the bias value in the dry season was smaller than in the wet and transitional seasons. All models performed well as shown by the low bias values except for the ACCESS1-0 RCP8.5 model. The findings revealed that MRI-CGCM was the best model for calibration, whereas EC-Earth was the best model in the validation period for both RCP4.5 and RCP8.5 scenarios. Further, the choice of climate model may influence water resource management over watershed scale.

KEYWORDS
bias correction, climate change, CORDEX, NEXGDPP, rainfall

INTRODUCTION

As the biggest equatorial archipelago country in the world, Indonesia is very vulnerable to climate change (Djalante, 2018; Paulus and Hindmarsh, 2018). Climate change affects various sectors in Indonesia, such as the economy, agriculture, infrastructure, and health, by increasing hydrometeorological disasters (floods, landslides, droughts, storms, and high sea waves). This will further decrease food production, increase damage to infrastructure and facilities, and cause loss of properties and life (Basuki et al., 2022; Mora et al., 2018; Noor and Maulud, 2022).

The Ciliwung watershed is one of the critical watersheds in Java. Therefore, it is vulnerable to climate change. The upstream of the Ciliwung watershed experienced extreme events in the future, by an increased peak discharge up to 130% in 2030 (Emam et al., 2016). In the downstream, such as in Jakarta, in 2050 the flood risk will increase by 322-402% due to climate change, land use change, and land subsidence (Budiyono et al., 2016; Januriyadi et al., 2018). The increased extreme rainfall will exacerbate the flood situation (Swain et al., 2020; Estiningtyas et al., 2009). Another study showed an increased flood

inundation in Jakarta by 6% (area) and 31% (depth) due to climate change (Mishra et al., 2018).

Rainfall is an essential variable in the water supply-demand calculations. Thus, it is crucial for water resource management (Sharafatmandrad and Mashizi, 2021; Yu et al., 2022) and disaster mitigation (Dhanesh et al., 2020; Nuryanto et al., 2020), especially to predict the occurrence of flood and drought events. The accuracy of water resource assessment is affected by the limited monitoring of rainfall at a finer spatial resolution, as it is mostly not measured except in a few stations. (Bhaga et al., 2020). CHIRPS has an advantage in terms of resolution, both spatial (5 km) and temporal (daily) resolution, and the data has also been available since 1981 (Funk et al., 2015). In addition, CHIRPS has proven to be quite good at describing observational data in several regions with different climates (Dhanesh et al., 2020; Wiwoho et al., 2021). Furthermore, rainfall is also an essential variable in climate change studies (Konapala et al., 2020).

Nowadays, there have been many studies of climate change impact on the increased extreme rainfall in Southeast Asia (Mandapaka and Lo, 2018; Raghavan et al., 2018; Supari et al., 2020; Tangang et al., 2018), which showed the necessity of high Climate

Model (RCM) output (Gutowski et al., 2020; Roberts et al., 2018). CORDEX SEA, as a consortium of several countries in the downscaling project, provides a model for regional climate prediction in the Southeast Asia region. Besides CORDEX, NEX-GDDP also provides the RCM data. Both CORDEX and NEX-GDDP data have a spatial resolution of 25 km at a daily temporal resolution.

Yet, the RCM climate model results have a bias value, which will further cause significant unreliability in projected rainfall (Raghavan et al., 2018). Furthermore, this can lead to inaccuracies in projected data that will influence the policy's decision making. Therefore, bias correction is required to minimize statistical bias in the output data (Racines et al., 2020).

This study aims to test the reliability of high-resolution climate model outputs by stochastic approach in representing rainfall conditions in the Ciliwung watershed. The statistical bias method in this study refers to the quantile mapping method, which relates the cumulative distribution function (CDF) values of rain observations and climate model (Inomata et al., 2011; Narulita et al., 2021; Racines et al., 2020).

RESEARCH METHODS

Data Source

This study focused on the Ciliwung watershed, which is geographically located at 6°11′ - 6°46′ S and 106°46′ - 107°00′ E (Figure 1). The watershed covers 347 km^2 with a river length of 117 km. Generally, the watershed is commonly divided into three parts based on the topography as upstream, middle, and downstream (Hermawan et al., 2019).

This study used CHIRPS daily rainfall data (http://chg.geog.ucsb.edu/data/chirps/) and has been corrected by observational data from the Meteorological, Climatological, and Geophysical Agency (BMKG) station. As projected data, this study used CORDEX data, which is available from the Center for Research and Development of BMKG and NEX-GDDP data, which is available from https://portal.nccs-.nasa.gov/datashare/ (Table 1). The available data was divided into two: the periods 1981-2005 for calibration and 2006-2020 for validation. The climate scenarios used during the validation period in this study were the RCP4.5 and RCP8.5 scenarios.

Data Correction

The corrected CHIRPS data was used to correct the RCM output data. The correction method used statistical bias correction based on the Quantile Map-
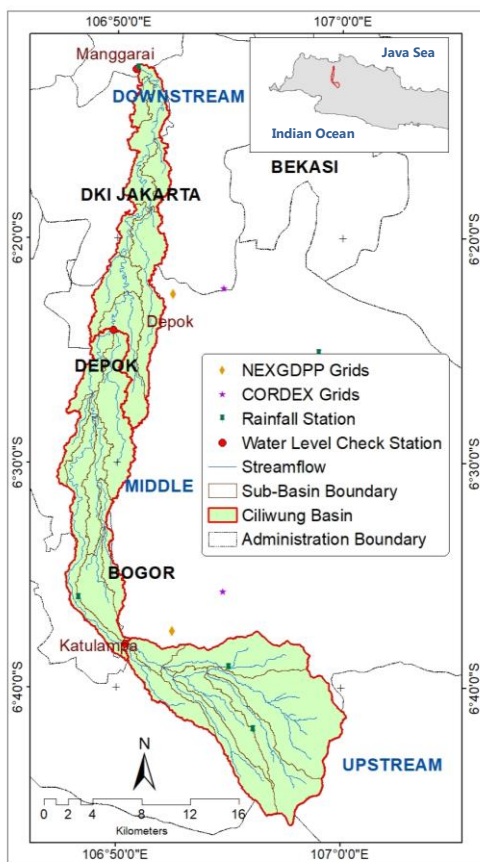
Figure 1. The location of Ciliwung watershed in West Java, Indonesia as indicated by a red polygon.

Table 1. The climate models used in the research.

	Climate Models	Abbreviation
CORDEX	Max Planck Institute for Meteorology	MPI
	Centre National de Recherches Météorologiques	CNRM-CM5
	EC-Earth consortium	EC-Earth
	Commonwealth Scientific and Industrial Research Organisation	CSIRO MK3.6
NEXGDPP	The Australian Community Climate and Earth System Simulator Coupled Model	ACCESS1-0
	Beijing Climate Center Climate System Model	BCC-CSM1-1
	Beijing Normal University Earth System Model	BNU-ESM
	Canadian Center for Climate Modelling and Analysis	CanESM2
	Community Climate System Model Version 4	CCSM4
	Community Earth System Model Biogeochemical Model	CESM1-BGC
	Institute of Numerical Mathematics Climate Model	INMCM4
	Model for Interdisciplinary Research on Climate-Earth System Model-Chemistry Component	MIROC-ESM-CHEM
	Meteorological Research Institute coupled GCM	MRI-CGCM
	The Norwegian Earth System Model	NorESM1

ping (QM). The QM method effectively eliminated bias between models and observations (Crochemore et al., 2016) and increased the reliability of model forecasts to some extent (Zhao et al., 2017). The correction was made based on a modification of the Inomata correction method (Narulita et al., 2021), which ignored zero rainfall values or the number of no-rain days on the Cumulative Distribution Function (CDF). Modifications in this method were based on the consideration that zero rainfall represents all segments in the CDF, whereas it means a non-entity for bias correction. The probability of exceedance was used in this method, Non-Exceedance Probability (NEP) ≥ 95% and non-NEP > 99.5%. NEP ≥ 99.5% of the CDF curve represents the limited extremes and excludes only a few outliers. However, CDFs with NEP ≥ 95% represent much better extremes than time series data.

The first step in this method was to calculate the correction factor for each quantile (αq, q = 0, 0.1, ..., 1) of the rainfall CDF, in which only non-zero rainfall values were used to construct the CDF. The correction coefficient was calculated between the corrected CHIRPS of the same rank and the RCM extremes extracted in the previous step (Equation 1). The calculation of the correction coefficient differentiated between extreme and non-extreme daily rainfall. The data segment with the largest 5% probability of all data was separated for extreme values. Next, extreme value correction coefficients were calculated for each quantile in this data segment. For non-extreme values, data was disaggregated and sorted monthly. Zero values of rainfall were excluded from the calculations. The coefficient of correction is the ratio of the corrected CHIRPS monthly non-extreme quantile value to the monthly RCM value. The obtained correction

coefficient was applied to the RCM rainfall data between the rainfall value in a quantile and the value below it to get the corrected RCM value (Equation 2).

$$a_q = \frac{R\_CHIRPScor_q}{R\_RCM_q} \qquad (1)$$

$$a_{qm} = \frac{R\_CHIRPScor_{qm}}{R\_RCM_{qm}} \qquad (2)$$

Where a_q is the correction coefficient of the q-th quantile, R_CHIRPScore$_q$ is the corrected CHIRPS rainfall value in the q-th quantile, R_RCM$_{qm}$ is the RCM rainfall value in the q-th quantile.

Model Assessments

Verification and validation of the corrected model output data were needed to assess the model's accuracy. Statistical model accuracy was calculated based on bias values (Equation 3) (Mokhtari et al., 2022), Mean Absolute Percentage Error (MAPE) (Equation 4), and Mean Square Error (MSE) (Equation 5). The model bias was also analyzed for each season, where December-January-February (DJF) is the wet month and June-July-August (JJA) is the dry month. The months of March-April-May (MAM) and September-October-November (SON) are included in the transition season.

The lower of bias, MSE, and MAPE values, the better of model accuracy and capability (Table 2).

$$bias = \frac{\sum_{i=1}^{n}(Obs_i - Sim_i)}{n} \qquad (3)$$

$$MSE = \frac{\sum_{i=1}^{n}[Obs - Sim]^2}{n} \qquad (4)$$

$$MAPE = \frac{\sum_{t=1}^{n}|(\frac{Obs - Sim}{Obs})100|}{n} \qquad (5)$$

Visually, the best model performance was determined by Taylor diagrams. The Taylor diagram

(a)

(b)
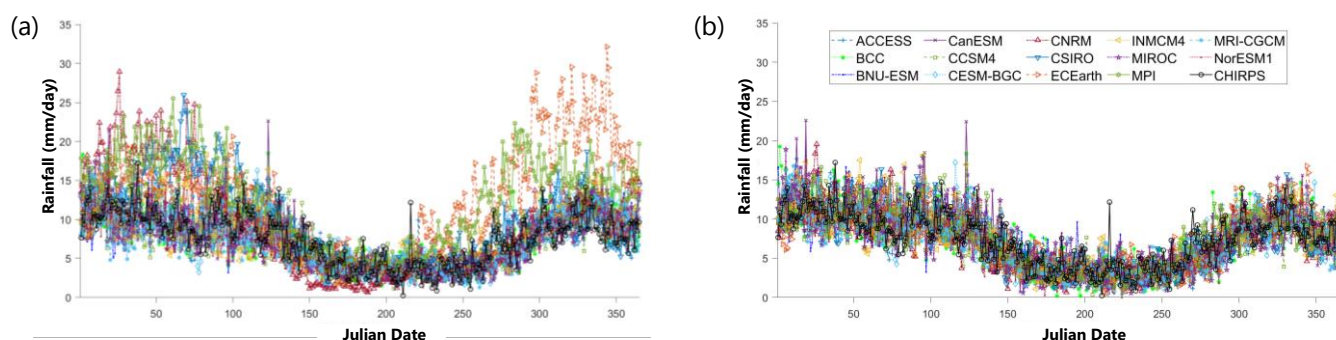
Figure 2. Daily mean rainfall of model and CHIRPS data (a) before and (b) after bias correction for 1981-2005.

serves to simplify how good the model was based on the correlation value (R), root-mean-square (RMSE), and standard deviation (Taylor, 2001). This diagram illustrates the performance of the model as well as the model performance ranking method (Handoko et al., 2019).

Table 2. The Mean Absolute Percentage Error (MAPE) criteria (Baykal et al., 2022).

MAPE	Criteria
<10%	Highly accurate
10-20%	Good
20-50%	Reasonable
>50%	Weak and inaccurate

RESULTS AND DISCUSSION

Historical Period (Calibration)

Before the bias correction, a comparison of observed daily average rainfall data from 1981-2005 with RCM rainfall data shows that the RCM data have significant variations (Figure 2a). During wet months, several CORDEX RCM models tended to have higher values than observations, including EC-Earth, CNRM-CM5, CSIRO MK3.6, and MPI. Conversely, during dry months, especially for the CNRM-CM5 model, the average daily rainfall was lower than the observed value. The highest observed daily average rainfall of 17.2 mm occurred on February 7th, while the highest rainfall from the RCM ranged from 15.7 – 32.1 mm. The highest value was the output of the EC-Earth model on December 10th.

The high rainfall variation of climate model output was also evident in the monthly average rainfall before correction (Figure 3a). Similar to the daily average rainfall, the four RCM CORDEX models produced higher rainfall than the observed rainfall, especially during the wet months. The maximum and minimum observed monthly average rainfall was

recorded at 347.5 mm in January and 110.3 mm in July. The EC-Earth model has the highest monthly average rainfall compared to other climate models, with 671.5 mm in November. In contrast, the minimum monthly average rainfall of 45.3 mm was produced by the CNRM-CM5 model in June.

The results of the statistical bias correction produced corrected rainfall values, which were close to observations, both daily average rainfall (Figure 2b) and monthly average rainfall (Figure 3b). Before the bias correction, the mean and standard deviation of the average daily rainfall of the RCM ranged from 7.1 – 12.5 mm and 3.1 – 6.5 mm. While the average value and standard deviation of the daily average rainfall CHIRPS ranged from 7.1 – 7.6 mm and 3.1 – 3.9 mm per day. The close of the standard deviation value between the observation and model data indicated that both have a similar pattern. The corrected maximum daily average rainfall ranged from 15.6 – 22.6 mm, where the CanESM2 model produced the highest maximum rainfall on May 3rd. Meanwhile, the maximum monthly average rainfall ranged from 314.5 – 382.3 mm.

Based on statistical parameters, negative bias values for all CORDEX RCM before correction indicated that the model was overestimated (Table 3). In contrast, the NEXGDPP RCM model produced underestimated rainfall values except for the CESM-BGC and INMCM4 models. While seasonally, bias values indicated that the RCM CORDEX was overestimated in each season before the correction process, except for the CNRM model in the dry season with a bias of 1.5 mm (Figure 4).

Yet, the RCM NEXGDPP rainfall was overestimated in the wet season and underestimated in the dry and transitional seasons. The model correction by adjusting the CDF value could reduce the rainfall bias up to 5.1 mm. Based on the MAPE value, statistical bias

(a)

(b)
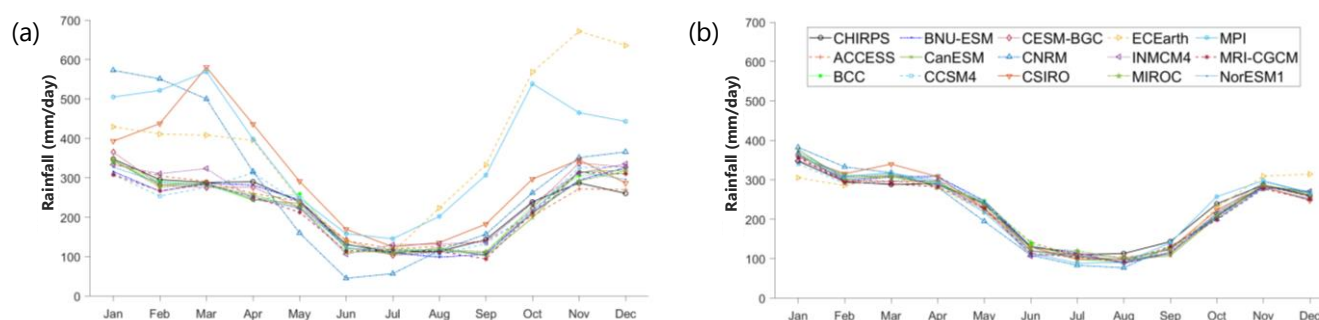
Figure 3. Monthly mean rainfall of model and CHIRPS data period 1981-2005 (a) before and (b) after bias correction.

correction also improved the performance of the CORDEX models (CNRM-CM5, CSIRO MK3.6, EC-Earth, and MPI) from the weak to the decent category.

Current Period (Validation)

Similar to the calibration period, the uncorrected RCM CORDEX rainfall during the validation period (2006 - 2020) tended to overestimate. Both RCP 4.5 and RCP 8.5 scenarios (Figure 5) resulted in high rainfall. In contrast, the RCM NEXGDPP average daily rainfall tended to be underestimated compared to the observation data, except for the ACCESS1-0 RCP8.5 model. The observed average daily rainfall had the highest value on November 29th at 18.5 mm for 15 years. The ACCESS1-0 model's output rainfall reached a maximum value on January 20th of 74.9 mm. This value was much greater than other models' average daily rainfall value. Monthly average rainfall also tended to be overestimated and has high fluctuations, especially detected in the RCM CORDEX output rainfall for RCP4.5, namely: CNRM-CM5, CSIRO MK3.6, EC-

Earth, and MPI. Specifically, the CNRM-CM5 model was overestimated in the wet season.

Statistical bias correction for the daily rainfall of the climate model in the validation period resulted in a relative value to the observed rainfall (Figure 5b and Figure 5d). However, the bias correction has not improved the ACCESS1-0 RCP8.5 daily rainfall. On the other hand, the average daily rainfall value has increased several times. Similar to the daily rainfall, the bias correction for the monthly rainfall increased the model performance, except for the ACCESS1-0 RCP8.5 model (Figure 5d). In January, the observed average monthly rainfall was 353.9 mm, while the ACCESS1-0 model's average monthly rainfall before correction reached 726.1 mm and increased to 800.6 mm after the bias correction.

The statistical parameters between the observed daily rainfall and the model's daily rainfall showed that the bias correction increased the model's performance (Table A1). The bias values of the output rainfall for the climate models RCP4.5 and RCP8.5 decreased by 4.5 mm and 4.8 mm, respectively. Yet, the bias value in the

Table 3. Comparison of statistical parameters between daily mean observed rainfall and historical RCM.

Model		Before Correction			After Correction		
		bias	MAPE	MSE	bias	MAPE	MSE
CORDEX	CNRM	-1.95	57.16	25.77	0.28	37.02	7.52
	CSIRO	-2.56	56.16	20.1	-0.03	34.7	6.46
	ECEarth	-5.02	97.34	55.46	0.07	39.77	6.95
	MPI	-4.82	89.04	41.05	-0.02	33.61	6.4
NEX-GDPP	ACCESS	0.11	38.96	6.98	0.15	37.27	7.1
	BCC	0.05	40.18	7.58	0.04	41.78	8.26
	BNU-ESM	0.23	36.57	7.33	0.03	39	8.01
	CanESM2	0.18	38.66	9.2	0.1	39.25	9.85
	CCSM4	0.06	36.75	8.06	0.25	35.07	7.27
	CESM1-BGC	-0.09	36.61	8.1	0.22	36.14	7.53
	INMCM4	-0.22	44.56	10.01	0.12	42.43	9.12
	MIROC	0.24	35.57	7.18	0.01	39.46	7.5
	MRI-CGCM	0.4	39.05	7.4	0.36	36.98	6.49
	NorESM1	0.22	34.98	6.79	-0.02	36.64	7.87
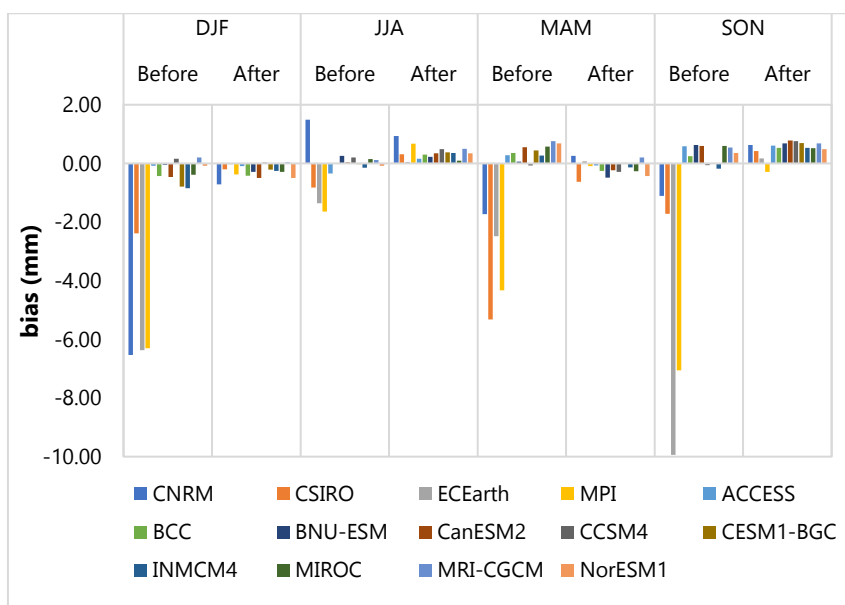
Figure 4. Seasonal bias values for CHIRPS data based on historical period for different RCM.

RCP4.5 scenario of the CESM-BGC and INMCM4 models has increased. This bias increase also occurred in the RCP 8.5 climate scenario for several climate models, including ACCESS1-0, CESM-BGC, MIROC-ESM-CHEM, and NorESM1-M. It was strengthened by most of the NEXGDPP RCM output MSE values increased after the bias correction. Nevertheless, the MSE of RCM CORDEX, namely CNRM-CM5, CSIRO MK3.6, EC-Earth, and MPI, decreased in both the RCP4.5 and RCP8.5 climate scenarios.

The negative bias values based on the RCM CORDEX seasonally showed that most models were overestimated each season (Figure A1). Conversely, the positive bias value was obtained for the CNRM model in dry months, both RCP4.5 and RCP8.5 scenarios (Figure A1c) and the transitional month of SON scenario RCP4.5 (Figure A1d). Most of the NEXGDPP RCM bias was positive in the wet and dry seasons, indicating that the model rainfall was mainly underestimated. During the transitional season, especially during the MAM, most of the NEXGDPP models were overestimated, while during the SON month, all models were underestimated. During the dry season, the bias values of all RCM models, both CORDEX and NEXGDPP, were smaller than the bias values in the wet and transitional seasons. In addition, bias correction improved model performance significantly for the CORDEX RCM. On the other hand, the performance of the NEXGDPP RCM after correction did not show a significant improvement.

The Model Comparison

The performance of the corrected RCM models was mathematically illustrated by a Taylor diagram (Fi-

gure 7). The best model will be located closest to the observation. Based on the proximity of the Taylor diagram to the calibration period, the CSIRO MK3.6, MPI, and MRI-CGCM3 models performed equally well. The three models have almost the same correlation to the observation of 0.7. Nevertheless, the MRI-CGCM model has the smallest RMSE values and standard deviations, 3.5 mm, and 2.5 mm. Therefore, the MRI-CGCM3 model was determined to have the best performance in the calibration period. In the validation period, both the RCP4.5 and RCP8.5 scenarios showed that the EC-Earth model has the best performance (Figure 6).

Each RCM has its characteristics. This caused different patterns of variation, both daily and monthly rainfall. The Ciliwung Watershed has a monsoonal pattern climate with one peak rainy season. This was clearly illustrated in the daily (Figure 2 and Figure 5) and monthly mean rainfall patterns (Figure 3 and Figure 6). However, there was a difference in magnitude between the RCM output and the observed rainfall. Same to the previous study by Raghavan et al., (2018), the NEXGDPP monthly rainfall over the calibration period has a good fit. Yet, this was not the case in the validation period, especially for RCM ACCESS1-0 for the RCP8.5 scenario.

Bias correction with the QM method effectively reduced the RCM bias value. All RCM outputs in the calibration period, especially CORDEX experienced significant performance improvement after the bias correction. Only the CCSM4 model has an increased bias value. Based on the MAPE value, all models in the calibration period was in the feasible category. Yet, the feasibility of the model during the validation period has largely declined after the bias correction. Only the ACCESS1-0, CNRM-CM5, EC-Earth, MPI, and NorESM1
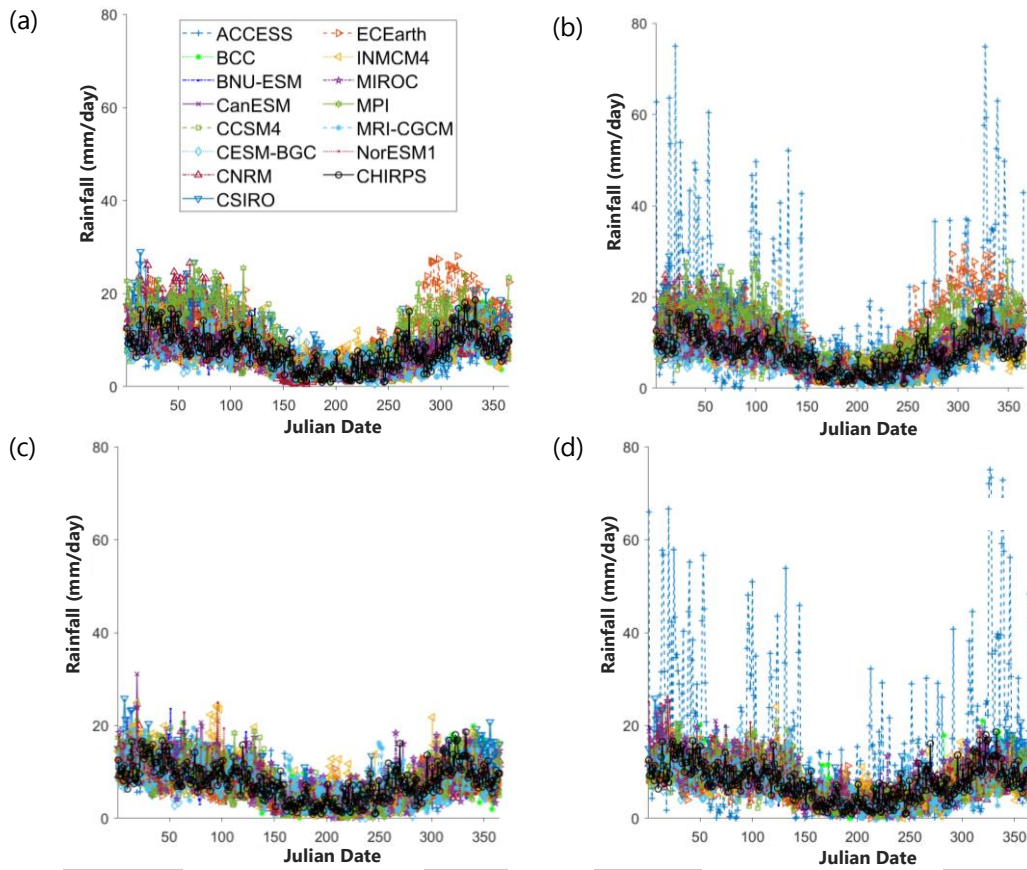
Figure 5. Comparison of daily observed CHIRPS rainfall with (a) the RCP4.5 before, (b) RCP8.5 before, (c) RCP4.5 after, and (d) RCP8.5 after bias correction for 2006-2020.
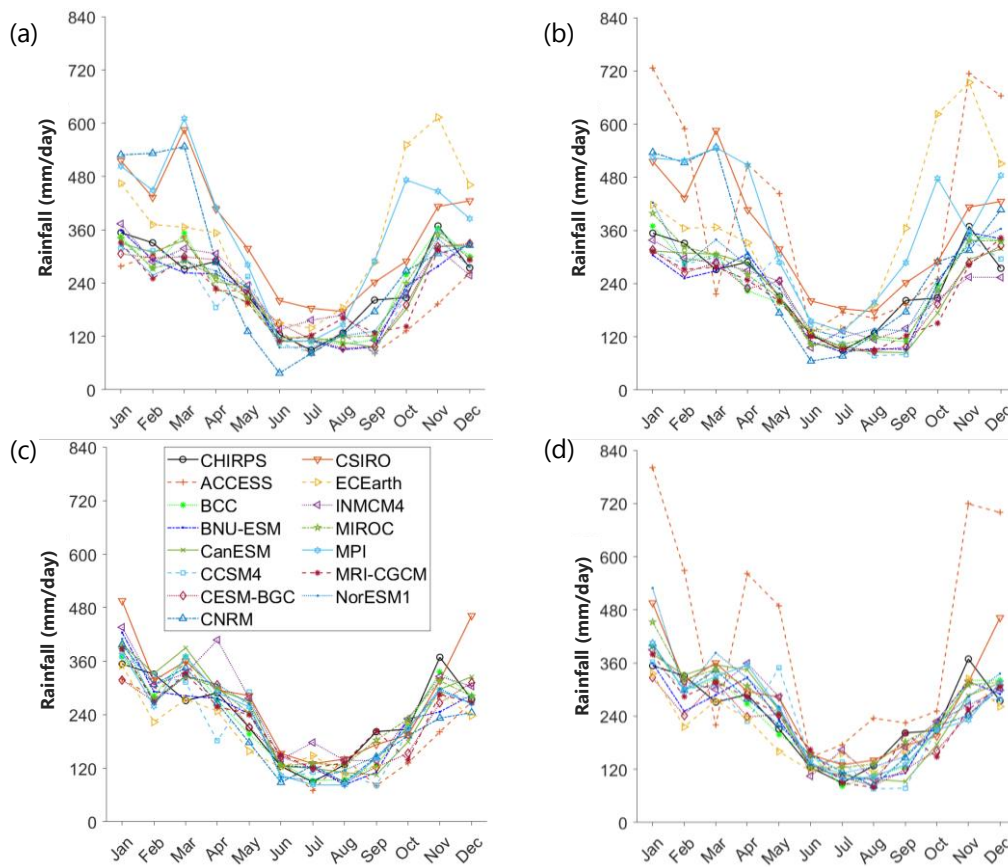
Figure 6. Comparison of monthly observed CHIRPS rainfall with (a) the RCP4.5 before, (b) RCP8.5 before, (c) RCP4.5 after, and (d) RCP8.5 after bias correction for 2006-2020.
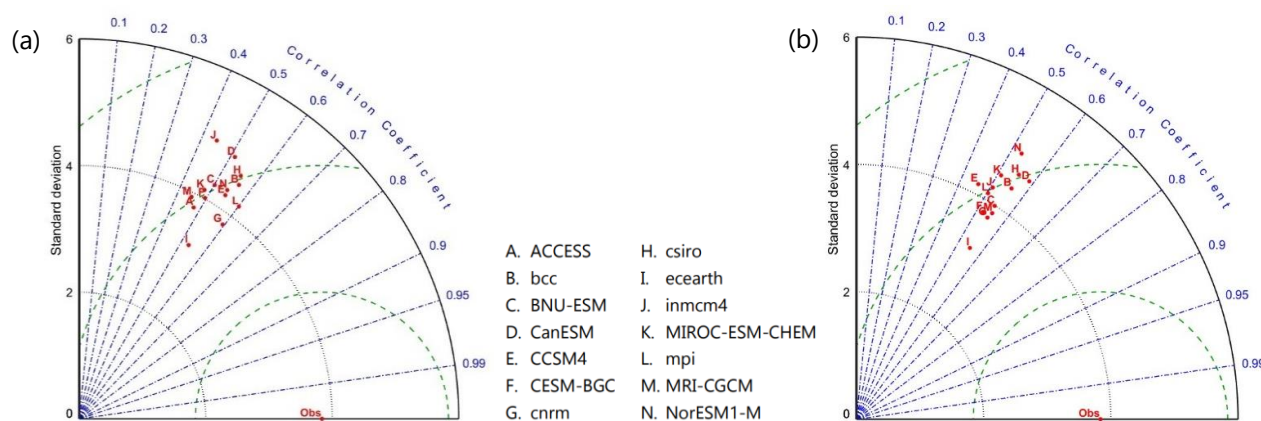
Figure 7. Taylor diagram of rainfall for (a) the RCP4.5 and (b) the RCP8.5 after correction.

models were eligible for scenario RCP4.5, while the BNU, CanESSM, CESM-BGC, CNRM-CM5, EC-Earth, MPI, and MRI-CGCM for the RCP8.5 scenario. In addition, the NEXGDPP RCM MSE value also tended to increase in this period. This showed that bias in the calibration period contributed to the large unreliability of projected rainfall values. Raghavan et al., (2018) and Maraun and Widmann, (2018) even stated that the validation process may have incorrect results. However, the bias correction results reflected the dynamics or internal variations of the RCM. Furthermore, Hall et al., (2019), analyzed the relationship of emerging constraints (EC) with observational data to reduce the unreliability of future climate models.

Based on the Taylor diagram, the model with the best performance for each period was different. During the calibration period, the best performance was MRI-CGCM, while EC-Earth was for the validation period. Furthermore, the RCM CORDEX rainfall was overestimated during the rainy season and underestimated during the dry season (Figure 2). It was because RCM has several factors that influence the output, including the variability of internal methods, regional or site studies, approaches, and downscaling configurations from the global model (GCM) to the regional model (RCM) (Gutowski et al., 2020), scenarios climate used (Deser et al., 2020), and as well known, the parameterization of each GCM model was built with different schemes, both microphysical, radiation, turbulence, and convective parameterization. Each of these parameterizations has a major influence on the resulting model output (Donahue and Caldwell, 2018).

RCM faced different challenges in every different driving factor (Djuwansah et al., 2021). For example, a past study on the Batanghari watershed showed ACCESS1-0 was the best model (Handoko et al., 2019). This was in contrast to the results of this study, where ACCESS1-0 has very poor performance, especially for

the RCP8.5 scenario. On the other hand, the seasons also affected the bias value (Kerkhoff et al., 2014).

CONCLUSIONS

The magnitude of daily and monthly rainfall data observed by CHIRPS tends to be lower than RCM CORDEX rainfall, while it is higher than NEX-GDPP rainfall. This indicates a bias between the observational data and the model. The bias values of all RCM models, both CORDEX and NEXGDPP in dry season are smaller the bias values in wet and transitional seasons. The model results were corrected using statistical bias correction, which showed a good enough result for most models except ACCESS1-0 RCP8.5. Bias correction using the QM method can reduce the model's rainfall bias up to 5.1 mm, 4.5 mm, and 4.8 mm in the calibration and validation periods of RCP4.5 and RCP8.5. The inaccuracy of performance between calibration and validation periods indicates that the validation process needs to be addressed. Based on the Taylor diagram, the model with the best performance in the historical period is the MRI-CGCM with the RMSE values and the smallest standard deviations of 3.5 mm and 2.5 mm. In the current period, for both RCP4.5 and RCP8.5 scenarios, EC-Earth is the best model.

REFERENCES

Basuki, T.M., Nugroho, H.Y.S.H., Indrajaya, Y., Pramono, I.B., Nugroho, N.P., Supangat, A.B., Indrawati, D.R., Savitri, E., Wahyuningrum, N., Purwanto,

Cahyono, S.A., Putra, P.B., Adi, R.N., Nugroho, A.W., Auliyani, D., Wuryanta, A., Riyanto, H.D., Harjadi, B., Yudilastyantoro, C., Hanindityasari, L., Nada, F.M.H., Simarmata, D.P., 2022. Improvement of Integrated Watershed Management in Indonesia for Mitigation and Adaptation to Climate Change: A Review. Sustainability 14, 9997. https://doi.org/10.3390/su14169997.

Bhaga, T.D., Dube, T., Shekede, M.D., Shoko, C., 2020. Impacts of Climate Variability and Drought on Surface Water Resources in Sub-Saharan Africa Using Remote Sensing: A Review. Remote Sensing 12, 4184. https://doi.org/10.3390/rs12244184.

Budiyono, Y., Aerts, J.C.J.H., Tollenaar, D., Ward, P.J., 2016. River flood risk in Jakarta under scenarios of future change. Natural Hazards and Earth System Sciences 16, 757–774. https://doi.org/-10.5194/nhess-16-757-2016.

Crochemore, L., Ramos, M.-H., Pappenberger, F., 2016. Bias correcting precipitation forecasts to improve the skill of seasonal streamflow forecasts. Hydrology and Earth System Sciences 20, 3601–3618. https://doi.org/ 10.5194/hess-20-3601-2016.

Deser, C., Lehner, F., Rodgers, K.B., Ault, T., Delworth, T.L., DiNezio, P.N., Fiore, A., Frankignoul, C., Fyfe, J.C., Horton, D.E., Kay, J.E., Knutti, R., Lovenduski, N.S., Marotzke, J., McKinnon, K.A., Minobe, S., Randerson, J., Screen, J.A., Simpson, I.R., Ting, M., 2020. Insights from Earth system model initial-condition large ensembles and future prospects. Nature Climate Change 10, 277–286. https://doi.org/10.1038/s41558-020-0731-2.

Dhanesh, Y., Bindhu, V.M., Senent-Aparicio, J., Brighenti, T.M., Ayana, E., Smitha, P.S., Fei, C., Srinivasan, R., 2020. A Comparative Evaluation of the Performance of CHIRPS and CFSR Data for Different Climate Zones Using the SWAT Model. Remote Sensing 12, 3088. https://doi.org/10.3390/rs12183088.

Djalante, R., 2018. Review article: A systematic literature review of research trends and authorships on natural hazards, disasters, risk reduction and climate change in Indonesia. Natural Hazards and Earth System Sciences 18, 1785–1810. https://doi.org/10.5194/nhess-18-1785-2018

Djuwansah, M.R., Narulita, I., Fajary, F.R., Mulyono, A., 2021. Rainfall data Similarity Assessment of the Coordinated Regional Downscaling Experiments South East Asia Models to Observation in the Bintan Island, in: IOP Conference Series: Earth and Environmental Science. IOP Publishing Ltd. https://doi.org/10-.1088/17551315/789/1/012051.

Donahue, A.S., Caldwell, P.M., 2018. Impact of Physics Parameterization Ordering in a Global Atmosphere Model. Journal of Advances in Modeling Earth Systems 10, 481–499. https://doi.org/10.1002/2017MS001067.

Emam, A.R., Mishra, B., Kumar, P., Masago, Y., Fukushi, K., 2016. Impact Assessment of Climate and Land-Use Changes on Flooding Behavior in the Upper Ciliwung River, Jakarta, Indonesia. Water 8, 559. https://doi.org/10.3390/w8120559.

Estiningtyas, W., Boer, R., Buono, A., 2009. Analysis of Relationship between Rainfall and Flood as well as Drought Events on Area With Rice Farming System In West Java Province. Agromet 23, 11-19. https://doi.org/10.29244/j.agromet.23.1.11-19.

Funk, C., Peterson, P., Landsfeld, M., Pedreros, D., Verdin, J., Shukla, S., Husak, G., Rowland, J., Harrison, L., Hoell, A., Michaelsen, J., 2015. The climate hazards infrared precipitation with stations—a new environmental record for monitoring extremes. Scientific Data 2, 150066. https://doi.org/10.1038/sdata.2015.66.

Gutowski, W.J., Ullrich, P.A., Hall, A., Leung, L.R., O'Brien, T.A., Patricola, C.M., Arritt, R.W., Bukovsky, M.S., Calvin, K.V., Feng, Z., Jones, A.D., Kooperman, G.J., Monier, E., Pritchard, M.S., Pryor, S.C., Qian, Y., Rhoades, A.M., Roberts, A.F., Sakaguchi, K., Urban, N., Zarzycki, C., 2020. The Ongoing Need for High-Resolution Regional Climate Models: Process Understanding and Stakeholder Information. Bulletin of the American Meteorological Society 101, E664–E683. https://doi.org/10.1175/BAMS-D-19-0113.1.

Hall, A., Cox, P., Huntingford, C., Klein, S., 2019. Progressing emergent constraints on future climate change. Nature Climate Change 9, 269–278. https://doi.org/10.1038/s41558-0190436-6.

Handoko, U., Boer, R., Aldrian, E., Latifah, A.L., Dasanto, B.D., Apip, A., Misnawati, M., 2019. Comparison Performance of the Multi-Regional Climate Model (RCM) in Simulating Rainfall and Air Temperature in Batanghari Watershed. Aceh International Journal of Science and Technology 8, 52–67. https://doi.org/10.13170/aijst.8.2.12340.

Hermawan, E., Sitorus, S.R.P., Tarigan, S.D., 2019. Spatial dynamics of land use change to hydrological response in the upstream of Ciliwung

Watershed, West Java Province, Indonesia. Advances in Environmental Sciences International Journal of the Bioflux Society 11, 122–132.

Inomata, H., Takeuchi, K., Fukami, K., 2011. Development of a Statistical Bias Correction Method for Daily Precipitation Data of GCM20. Journal of Japan Society of Civil Engineers, Ser. B1 (Hydraulic Engineering) 67, I_247-I_252. https://doi.org/10.2208/jscejhe.67.I_247.

Januriyadi, N.F., Kazama, S., Moe, I.R., Kure, S., 2018. Evaluation of future flood risk in Asian megacities: a case study of Jakarta. Hydrological Research Letters 12, 14–22. https://doi.org/10.3178/hrl.12.14.

Kerkhoff, C., Künsch, H.R., Schär, C., 2014. Assessment of Bias Assumptions for Climate Models. Journal of Climate 27, 6799–6818. https://doi.org/10.1175/JCLI-D-13-00716.1.

Konapala, G., Mishra, A.K., Wada, Y., Mann, M.E., 2020. Climate change will affect global water availability through compounding changes in seasonal precipitation and evaporation. Nature Communications 11, 3044. https://doi.org/10.1038/s41467-020-16757-w.

Mandapaka, P.V., Lo, E.Y.M., 2018. Assessment of future changes in Southeast Asian precipitation using the NASA Earth Exchange Global Daily Downscaled Projections data set. International Journal of Climatology 38, 5231–5244. https://doi.org/10.1002/joc.5724.

Maraun, D., Widmann, M., 2018. Cross-validation of bias-corrected climate simulations is misleading. Hydrology and Earth System Sciences 22, 4867–4873. https://doi.org/10.5194/hess-22-4867-2018.

Mishra, B.K., Rafiei Emam, A., Masago, Y., Kumar, P., Regmi, R.K., Fukushi, K., 2018. Assessment of future flood inundations under climate and land use change scenarios in the Ciliwung River Basin, Jakarta. Journal of Flood Risk Management 11, S1105–S1115. https://doi.org/10.1111/jfr3.12311.

Mokhtari, S., Sharafati, A., Raziei, T., 2022. Satellite-based streamflow simulation using CHIRPS satellite precipitation product in Shah Bahram Basin, Iran. Acta Geophysica 70, 385–398. https://doi.org/10.1007/s11600-021-00724-0.

Mora, C., Spirandelli, D., Franklin, E.C., Lynham, J., Kantar, M.B., Miles, W., Smith, C.Z., Freel, K., Moy, J., Louis, L.V., Barba, E.W., Bettinger, K., Frazier, A.G., Colburn IX, J.F., Hanasaki, N., Hawkins, E., Hirabayashi, Y., Knorr, W., Little, C.M., Emanuel, K., Sheffield, J., Patz, J.A., Hunter, C.L., 2018. Broad threat to humanity from cumulative climate hazards intensified by greenhouse gas emissions. Nature Climate Change 8, 1062–1071. https://doi.org/10.1038/s41558-018-0315-6.

Narulita, I., Fajary, F.R., Syahputra, M.R., Kusratmoko, E., Djuwansah, M.R., 2021. Spatio-temporal rainfall variability of equatorial small island: case study Bintan Island, Indonesia. Theoretical and Applied Climatology 144, 625–641. https://doi.org/10.1007/s00704-021-03527-x.

Noor, N.M., Maulud, K.N.A., 2022. Coastal Vulnerability: A Brief Review on Integrated Assessment in Southeast Asia. Journal of Marine Science and Engineering 10, 595. https://doi.org/10.3390/jmse10050595.

Nuryanto, D.E., Fajariana, Y., Pradana, R.P., Anggraeni, R., Badri, I.U., Sopaheluwakan, A., 2020. Modeling of Heavy Rainfall Triggering Landslide Using WRF Model. J.Agromet 34, 55–65. https://doi.org/10.29244/j.agromet.34.1.55-65.

Paulus, R.Y., Hindmarsh, R., 2018. Addressing inadequacies of sectoral coordination and local capacity building in Indonesia for effective climate change adaptation. Climate and Development 10, 35–48. https://doi.org/10.1080/17565529.2016.1184609.

Racines, C.N., Tarapues, J., Thornton, P., Jarvis, A., Villegas, J.R., 2020. High-resolution and bias-corrected CMIP5 projections for climate change impact assessments. Scientific Data 7, 7. https://doi.org/10.1038/s41597-019-0343-8.

Raghavan, S.V., Hur, J., Liong, S.-Y., 2018. Evaluations of NASA NEX-GDDP data over Southeast Asia: present and future climates. Climatic Change 148, 503–518. https://doi.org/10.1007/s10584-018-2213-3.

Roberts, M.J., Vidale, P.L., Senior, C., Hewitt, H.T., Bates, C., Berthou, S., Chang, P., Christensen, H.M., Danilov, S., Demory, M.-E., Griffies, S.M., Haarsma, R., Jung, T., Martin, G., Minobe, S., Ringler, T., Satoh, M., Schiemann, R., Scoccimarro, E., Stephens, G., Wehner, M.F., 2018. The Benefits of Global High Resolution for Climate Simulation: Process Understanding and the Enabling of Stakeholder Decisions at the Regional Scale. Bulletin of the American Meteorological Society 99, 2341–2359. https://doi.org/10.1175/BAMS-D-15-00320.1.

Sharafatmandrad, M., Mashizi, A.K., 2021. Temporal and Spatial Assessment of Supply and Demand of the Water-yield Ecosystem Service for Water Scarcity Management in Arid to Semi-arid

Ecosystems. Water Resources Management 35, 63–82. https://doi.org/10.1007/s11269-020-02706-1.

Supari, Tangang, F., Juneng, L., Cruz, F., Chung, J.X., Ngai, S.T., Salimun, E., Mohd, M.S.F., Santi-sirisomboon, J., Singhruck, P., PhanVan, T., Ngo-Duc, T., Narisma, G., Aldrian, E., Gunawan, D., Sopaheluwakan, A., 2020. Multi-model projections of precipitation extremes in Southeast Asia based on CORDEX-Southeast Asia simulations. Environmental Research 184, 109350.
https://doi.org/10.1016/j.envres.2020.109350

Swain, D.L., Wing, O.E.J., Bates, P.D., Done, J.M., Johnson, K.A., Cameron, D.R., 2020. Increased Flood Exposure Due to Climate Change and Population Growth in the United States. Earth's Future 8. https://doi.org/10.1029/2020EF001778.

Tangang, F., Supari, S., Chung, J.X., Cruz, F., Salimun, E., Ngai, S.T., Juneng, L., Santisirisomboon, Jerasorn, Santisirisomboon, Jaruthat, Ngo-Duc, T., Phan-Van, T., Narisma, G., Singhruck, P., Gunawan, D., Aldrian, E., Sopaheluwakan, A., Nikulin, G., Yang, H., Remedio, A.R.C., Sein, D., Hein-Griggs, D., 2018. Future changes in annual precipitation extremes over Southeast Asia under global warming of 2°C. APN Science Bulletin 8. https://doi.org/10.30852/sb.2018.436.

Taylor, K.E., 2001. Summarizing multiple aspects of model performance in a single diagram. Journal of Geophysical Research: Atmospheres 106, 7183–7192. https://doi.org/10.1029/2000JD900719.

Wiwoho, B.S., Astuti, I.S., Alfarizi, I.A.G., Sucahyo, H.R., 2021. Validation of Three Daily Satellite Rainfall Products in a Humid Tropic Watershed, Brantas, Indonesia: Implications to Land Characteristics and Hydrological Modelling. Hydrology 8, 154. https://doi.org/10.3390/hydrology8040154.

Yu, Y., Zhou, T., Zhao, R., Li, Z., Shen, C., 2022. A scenario analysis-based optimal management of water resources supply and demand balance: A case study of Chengdu, China. PLOS ONE 17, e0267920.
https://doi.org/10.1371/journal.pone.0267920

Zhao, T., Bennett, J.C., Wang, Q.J., Schepen, A., Wood, A.W., Robertson, D.E., Ramos, M.-H., 2017. How Suitable is Quantile Mapping For Postprocessing GCM Precipitation Forecasts? Journal of Climate 30, 3185–3196. https://doi.org/10.1175/JCLI-D-16-0652.1.

ANNEX

Table A1. Statistical parameters between daily mean observed rainfall and RCM output before and after bias correction in the 2006-2020 period for RCP 4.5 (top panel) and RCP 8.5 (below panel).

	Model	RCP4.5					
		Before			After		
		Bias	MAPE	MSE	Bias	MAPE	MSE
CORDEX	CNRM	-1.36	56.2	25.77	0.66	43.6	12.32
	CSIRO	-3.67	80.62	31.39	-1.29	54.34	18.04
	ECEarth	-3.52	82.64	37.96	0.97	49.51	12.91
	MPI	-3.75	75.09	37.83	0.31	45.22	13.06
NEX-GDPP	ACCESS	1.29	45.27	15.74	0.98	48.99	16.22
	BCC	0.27	46.3	13.24	0.22	50.45	15.42
	BNU-ESM	0.56	43.79	13.92	0.36	50.26	16.64
	CanESM2	0.37	47.79	14.53	-0.26	56.82	19.06
	CCSM4	0.6	45.99	13.9	0.54	50.24	15.1
	CESM1-BGC	0.41	50.96	15.08	0.57	54.41	15.92
	INMCM4	-0.09	60.32	17.88	-0.99	68.14	23.06
	MIROC	0.39	46.31	12.23	-0.2	59.7	16.56
	MRI-CGCM	0.76	49.16	14.77	0.18	54.26	16.56
	NorESM1	0.53	41.57	12.11	0.13	46.9	15.31

	Model	RCP8.5					
		Before			After		
		Bias	MAPE	MSE	Bias	MAPE	MSE
CORDEX	CNRM	-1.85	57.59	26.53	0.14	47.11	13.2
	CSIRO	-3.67	80.62	31.39	-1.29	54.34	18.04
	ECEarth	-4.09	88.52	48.48	0.75	45.63	12.01
	MPI	-4.45	90.07	45.21	-0.05	49.18	15.72
NEX-GDPP	ACCESS	-5.78	136.4	213.37	-6.73	159.25	254.35
	BCC	0.25	46.24	12.81	0.14	51.98	15.1
	BNU-ESM	0.53	43.65	12.84	0.32	49.65	14.1
	CanESM2	0.74	40.17	11.89	-0.03	49.73	15.21
	CCSM4	0.4	49.06	15.65	0.3	55.41	17.41
	CESM1-BGC	0.81	44.27	14.21	0.92	46.48	14.84
	INMCM4	0.6	49.03	13.46	-0.35	56.8	16.24
	MIROC	0.05	45.9	13.53	-0.63	57.42	17.51
	MRI-CGCM	0.94	41.97	12.51	0.28	48.36	13.45
	NorESM1	-0.46	51.97	13.87	-0.83	56.6	19.61

Figure A1. Statistical parameters between daily mean observed rainfall and RCM output before and after bias correction in the 2006-2020 period.